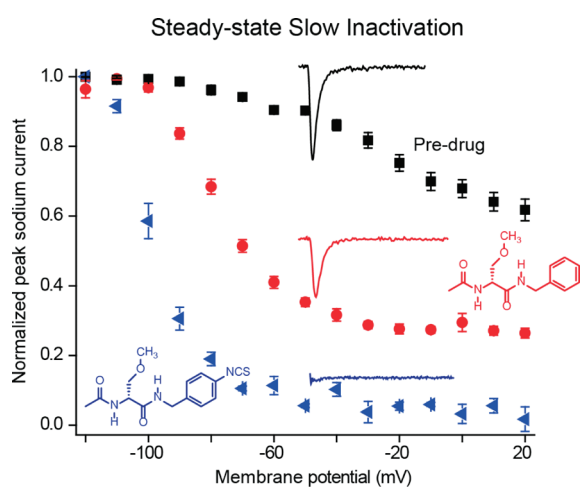


Development and Characterization of Novel Derivatives of the Antiepileptic Drug Lacosamide That Exhibit Far Greater Enhancement in Slow Inactivation of Voltage-Gated Sodium Channels

Yuying Wang,[†] Ki Duk Park,[‡] Christophe Salomé,[‡] Sarah M. Wilson,[‡] James P. Stables,[#] Rihe Liu,^{||} Rajesh Khanna,^{*,†,‡} and Harold Kohn^{*,§,‡}

[†]Departments of Pharmacology and Toxicology, [‡]Program in Medical Neuroscience, Paul and Carole Stark Neurosciences Research Institute, Indiana University School of Medicine, Indianapolis, Indiana 46202, United States, [§]Department of Chemistry, ^{||}Carolina Center for Genome Sciences, and [‡]Division of Medicinal Chemistry and Natural Products, UNC Eshelman School of Pharmacy, University of North Carolina, Chapel Hill, North Carolina 27599, United States, and [#]Epilepsy Branch, National Institute of Neurological Disorders and Stroke, National Institutes of Health, 6001 Executive Boulevard, Suite 2106, Rockville, Maryland 20892, United States

Abstract



The novel antiepileptic drug (*R*)-*N*-benzyl 2-acetamido-3-methoxypropionamide ((*R*)-lacosamide, Vimpat ((*R*)-1)) was recently approved in the United States and Europe for adjuvant treatment of partial-onset seizures in adults. (*R*)-1 preferentially enhances slow inactivation of voltage-gated Na⁺ currents, a pharmacological process relevant in the hyperexcitable neuron. We have advanced a strategy to identify lacosamide binding partners by attaching affinity bait (AB) and chemical reporter (CR) groups to (*R*)-1 to aid receptor detection and isolation. We showed that select lacosamide AB and AB&CR derivatives exhibited excellent activities similar to (*R*)-1 in the maximal electroshock seizure model in rodents. Here, we examined the effect of these lacosamide AB and AB&CR derivatives and compared them with (*R*)-1 on Na⁺ channel function in central nervous system (CNS) catecholaminergic (CAD) cells. Using whole-cell patch clamp electrophysiology, we demonstrated that the test compounds do not affect the Na⁺ channel fast inactivation process, that they were far better modulators of slow inactivation than (*R*)-1,

and that modulation of the slow inactivation process was stereospecific. The lacosamide AB agents that contained either an electrophilic isothiocyanate ((*R*)-5) or a photolabile azide ((*R*)-8) unit upon AB activation gave modest levels of permanent Na⁺ channel slow inactivation, providing initial evidence that these compounds may have covalently reacted with their cognate receptor(s). Our findings support the further use of these agents to delineate the (*R*)-1-mediated Na⁺ channel slow inactivation process.

Keywords: Lacosamide, sodium channel, slow inactivation, affinity bait

Epilepsy, a major neurological disorder that affects all populations (1), describes the types of recurrent seizures produced by paroxysmal, excessive neuronal discharges in the brain (2, 3). The mainstay of treatment for epileptic disorders has been the long-term and consistent administration of anticonvulsant drugs (4–8). Monotherapy, however, fails for one of every two patients with newly diagnosed epilepsy (9, 10). Of greater importance, current medications are ineffective for approximately one-third of patients with epilepsy (11–14). Many continue to have seizures, while others experience disturbing side effects (e.g., drowsiness, dizziness, nausea, liver damage) (15). The shortcomings of current regimens highlight the need for new antiepileptic drugs (AEDs) with novel mechanisms of action. Unfortunately, the inability to identify specific nervous system pathways and protein target sites responsible for seizures and seizure protection has hampered new drug development.

We discovered the novel AED (*R*)-*N*-benzyl 2-acetamido-3-methoxypropionamide (16) ((*R*)-lacosamide,

Received Date: September 27, 2010

Accepted Date: November 10, 2010

Published on Web Date: November 24, 2010

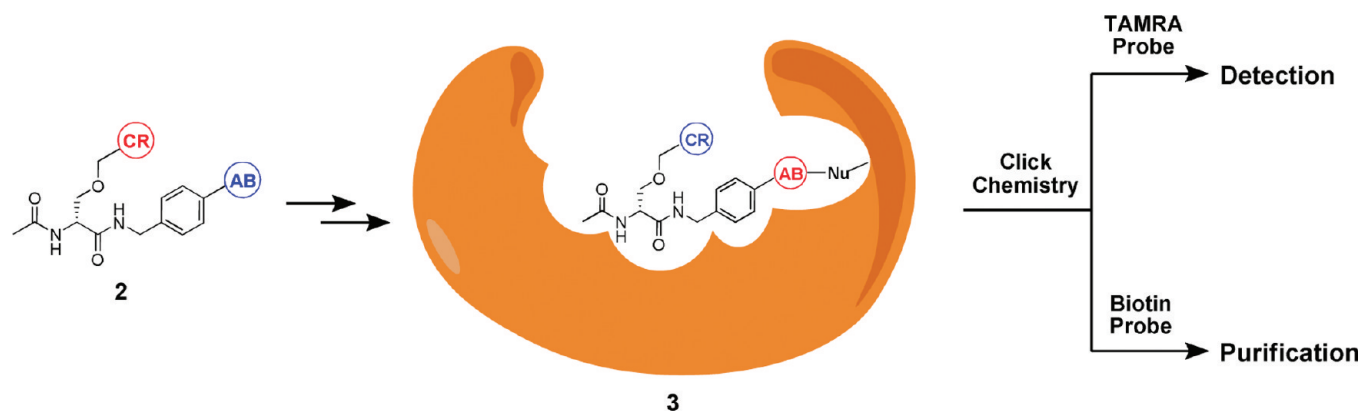
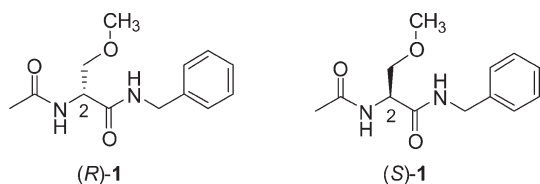


Figure 1. Use of the AB&CR strategy to identify potential drug receptors. Scheme showing the binding of lacosamide AB&CR (**2**) to a putative receptor. Initial binding provides a complex that permits covalent adduction through the AB moiety to give **3**. Protein detection is accomplished by reacting with a fluorescent probe containing an azide moiety by Cu(I)-mediated cycloaddition. Correspondingly, reacting **3** with a biotinylated probe containing an azide moiety allows receptor isolation using streptavidin.

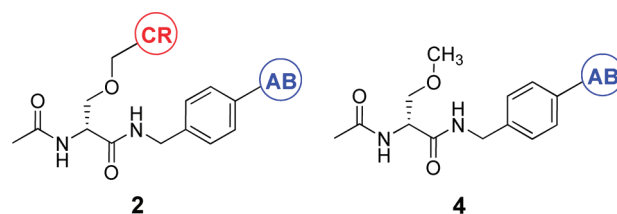
(*R*)-**1**). (*R*)-**1** was recently approved in the United States and Europe for adjuvant treatment of partial-onset seizures in adults (17). We reported on (*R*)-**1** for the control of convulsive disorders (16), determined the structure–activity relationship (SAR) of (*R*)-**1** (18, 19), and showed that anticonvulsant activity for this AED is stereospecific (16, 18). Whole animal pharmacological studies demonstrated that (*R*)-**1** function is unique and prevents seizure spread by mechanisms different from current and emerging clinical agents (20).



Electrophysiology experiments documented that (*R*)-**1** selectively enhanced slow inactivation of voltage-gated Na⁺ channels (VGSCs), a pharmacological site relevant in the hyperexcitable neuron (21, 22). In neuroblastoma cells, (*R*)-**1** enhanced Na⁺ channel slow inactivation in a time- and voltage-dependent manner, without affecting fast inactivation (21). (*R*)-**1** shifted the slow inactivation voltage curve to more hyperpolarized potentials and enhanced the maximal fraction of channels that were slowly inactivated. The slow inactivation process by (*R*)-**1** was stereoselective, with (*R*)-**1** being active but (*S*)-**1** not (21). Whole-cell, patch-clamp electrophysiology was also used to determine the effects of (*R*)-**1** on recombinant Na_v1.3 and Na_v1.7 channels expressed in HEK293 cells and on Na_v1.8-type tetrodotoxin-resistant currents recorded from small-diameter adult DRG neurons (22). Employing various (*R*)-**1** concentrations, (*R*)-**1** substantially reduced Na⁺ currents and enhanced only the voltage-dependence of steady-state slow inactivation (22). (*R*)-**1**

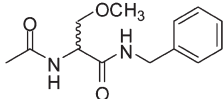
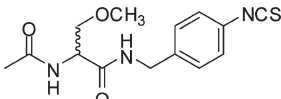
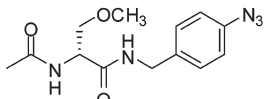
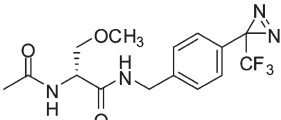
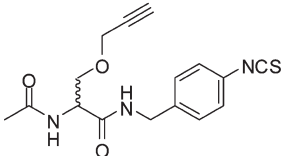
is the only known AED that selectively enhances slow inactivation without apparent interaction with fast inactivation gating (21, 22). Overall, these findings indicate that (*R*)-**1** reduces pathological activity of neurons (e.g., prolonged depolarizations in the hyperexcitable neuron) without disrupting normal physiological activity.

We have advanced a general strategy to identify targets of (*R*)-**1** function (23). Our approach used compounds termed (*R*)-**1** AB&CR agents ((*R*)-**2**), where AB stands for affinity bait and CR for chemical reporter (Figure 1). The AB group in (*R*)-**2** permits irreversible adduction of the modified drug to the receptor to give **3**, and the CR unit allows protein detection and capture upon subsequent attachment to a chemical probe (P). Incorporating AB and CR moieties within the (*R*)-**1** framework such that neither impedes drug binding to the cognate receptor(s) is key to this method's success.



In this study, we examined the effect of **1**, **2**, and lacosamide AB derivatives (**4**) on Na⁺ channel function in central nervous system (CNS) catecholaminergic (CAD) cells (24). We show that CAD cells serve as excellent, readily accessible surrogates for neuronal cells to examine drug interactions that affect Na⁺ channels. We demonstrate that (*R*)-**2** and (*R*)-**4** are *more effective* than (*R*)-**1** in selectively modulating Na⁺ channel slow inactivation processes in CAD cells, thus documenting that placement of select AB and CR moieties within the (*R*)-**1** framework did not disrupt the function of these agents.

Table 1. Anticonvulsant and Patch Clamp Electrophysiology Data for Lacosamide, Lacosamide-AB, and Lacosamide AB&CR Agents

Cpmd No.	Whole Animal Behavioral Studies				IC ^f value (μM)
	Mice (ip) ^a		Rat (po) ^d		
	MES, ^b ED ₅₀	Tox, ^c TD ₅₀	MES, ^b ED ₅₀	Tox, ^e TD ₅₀	
 (R)-1 ^g	4.5 [0.5] (3.7 – 5.5)	27 [0.25] (26 – 28)	3.9 [0.5] (2.6 – 6.2)	>500 [0.5]	85
(S)-1 ^g	>100, <300	>300	>30	>30	>1000
 (R)-5 ^h	24 [0.5] (21 – 27)	47 [0.25] (43 – 50)	4.2 [4] (2.4 – 8.0)	>250	8.1
(S)-5 ^h	>100, <300	>30, <100	>180	>30	68
 (R)-6 ⁱ	8.4 [0.25] (5.7 – 12)	46 [0.25] (41 – 52)	3.9 [0.5] (2.5 – 6.2)	>250	22
 (R)-7	15 [0.15] (14 – 16)	67 [0.25] (38 – 78)	<30 [0.5]	>30 [0.5]	12
 (R)-8 ^h	45 [1] (42 – 48)	110 [0.25] (76 – 150)	>30	>30	16
(S)-8 ^h	>300	>300	ND ^j	ND ^j	>200
phenytoin ^k	9.5 [2.0] (8.1 – 10)	66 [2.0] (53 – 72)	30 [4.0] (22 – 39)	/	NS ^{m,n}
phenobarbital ^k	22 [1.0] (15 – 23)	69 [0.5] (63 – 73)	9.1 [5.0] (7.6 – 12)	61 [0.5] (44 – 96)	NS ^m
valproate ^k	270 [0.25] (250 – 340)	430 [0.25] (370 – 450)	490 [0.5] (350 – 730)	280 [0.5] (190 – 350)	NS ^m

^a The compounds were administered intraperitoneally. ED₅₀ and TD₅₀ values are in milligrams per kilogram. Numbers in parentheses are 95% confidence intervals. The dose effect was obtained at the time of peak effect (indicated in hours in brackets). ^b MES = maximal electroshock seizure test. ^c TD₅₀ value determined from the rotarod test. ^d The compounds were administered orally. ED₅₀ and TD₅₀ values are in milligrams per kilogram. ^e Tox = behavioral toxicity. ^f IC₅₀, Concentration at which half of the Na⁺ channels have transitioned to a slow inactivated state. ^g Reference 16. ^h Reference 25. ⁱ Reference 26. ^j ND, not determined. ^k Reference 41. ^l No ataxia observed up to 3000 mg/kg. ^m NS, not selective for slow inactivation. ⁿ References 21 and 57.

We further report that modulation of Na⁺ channel slow inactivation by these agents is stereospecific and that the level of stereospecificity is similar to that observed in whole animal, behavioral seizure models (16, 18). CAD cells treated with **4** under conditions that led to AB utilization showed modest levels of permanent Na⁺ channel slow inactivation.

Results and Discussion

Choice of Compounds

Eight compounds were selected for study in CAD cells. (R)-1 and its stereoisomer, (S)-1, served as the parent compounds. We compared (R)-1 and (S)-1 on CAD cell sodium channel function with previous results

obtained in neuroblastoma cells (21). Next, we selected three (R)-4 agents wherein the AB moiety was incorporated at the benzyl amide 4'-site ((R)-5–(R)-7) (Table 1). We have reported that 4'-aryl substitution of (R)-1 provided compounds with exceptional anticonvulsant activity in the maximal electroshock (MES) seizure model (25) in rodents but that structural constraints for maximal activity existed for this substituent (18). Electrophilic (isothiocyanate (R)-5)(25) and photolabile (azide (R)-6 (26), (trifluoromethyl)diazirine (R)-7) AB groups were evaluated. Both AB types have been used in target modification studies (27–31). We included the (R)-1 AB&CR agent, (R)-8, in which the AB group was an isothiocyanate and the CR group was an alkyne unit. We have reported that replacing the 3-methoxy group in (R)-1

with a propargyloxy moiety provided a lacosamide derivative with excellent activity in the MES test (19, 25, 26). Moreover, the alkyne group in (*R*)-**8** readily undergoes [3 + 2] copper(I)-mediated cycloaddition with azide probes (click chemistry) (31–34). For compounds **1**, **5**, and **8**, we also tested the corresponding stereoisomer.

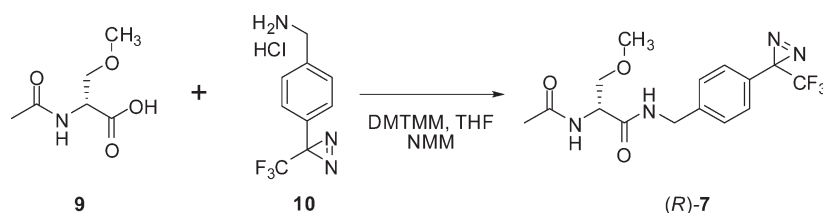
Synthesis

We have reported the stereospecific syntheses of **1** (16), **5** (35), **6** (26), and **8** (25). Compound **7** was prepared by coupling (*R*)-2-acetamido-3-methoxypropionic acid (36) (**9**) with 4-[3-(trifluoromethyl)-3H-diazirin-3-yl]-benzylmethanamine (**10**) (37) using 4-(4,6-dimethoxy-1,3,5-triazin-2-yl)-4-methoxymorpholinium chloride (DMTMM) (38) (Scheme 1). The enantiopurity of (*R*)-**7** was determined with the chiral-resolving agent (–)-mandelic acid (39).

Whole Animal Pharmacological Activity

Compounds (*R*)-**1**, (*S*)-**1**, (*R*)-**5**, (*S*)-**5**, (*R*)-**6**, (*R*)-**7**, (*R*)-**8**, and (*S*)-**8** were tested for anticonvulsant activity at the Anticonvulsant Screening Program (ASP) at the National Institute of Neurological Disorders and Stroke (NINDS), U.S. National Institutes of Health. Screening was performed using the procedures described by Stables and Kupferberg (40). The pharmacological data from the MES test (24) are summarized in Table 1, and similar results were obtained for the clinical AEDs phenytoin (41), valproate (41), and phenobarbital (41). All compounds were administered intraperitoneally (ip) to mice and orally (po) to rats. Table 1 lists the values from the rodent identification studies determined to be protective in blocking hind limb extension induced in the MES seizure model. For compounds that showed significant activity, we report the 50% effective dose (ED₅₀) values obtained in quantitative screening evaluations. Also provided are the median doses for 50% neurological impairment (TD₅₀) in mice, using the rotorod test (42), and the behavioral toxicity effects observed in rats (43). TD₅₀ values were determined for those compounds that exhibited significant activity in the MES test. When the lacosamide derivatives were evaluated in the subcutaneous Metrazol (scMet) seizure model (44), none provided protection at doses up to 300 mg/kg at two time points (0.5 and 4 h) (data not shown). The absence of seizure protection in this assay is a hallmark of this class of compounds (16, 18, 19).

Scheme 1. Synthesis of (*R*)-**7**



Compounds **1** and **5–8** all exhibited pronounced seizure protection in the MES test in both mice (ip) and rats (po) when the stereochemical configuration of the C(2) chiral center corresponded to the D-amino acid ((*R*)-configuration). In mice, we observed a 2–10-fold loss of activity compared with (*R*)-**1** upon incorporation of either an AB moiety (**4–7**) or both an AB and CR group (**8**) (16). While the whole animal pharmacological data do not permit us to identify the factors (e.g., effectiveness of the agent, metabolic factors, CNS bioavailability) that contributed to the modest loss of anticonvulsant activity, we found that incorporating the AB and CR moieties did not markedly alter the activity of these compounds in the MES test or the requirement for the D-amino acid configuration for activity seen for **1** (16).

Lacosamide Derivatives Inhibit Na⁺ Currents

Using the whole-cell patch clamp configuration, the effects of (*R*)-**1** and its derivatives, (*R*)-**5–(R)**-**8**, on voltage-gated Na⁺ channels were examined in CAD cells. CAD cells were chosen because they have a neuronal origin and express endogenous tetrodotoxin-sensitive Na⁺ currents with rapid activation and inactivation upon membrane depolarization (45, 46). Real-time quantitative PCR (qRT-PCR) of CAD cells revealed the presence of relatively high levels of Na_v1.7 mRNA (Figure 2, Table 2). Compared with Na_v1.7, lower levels of Na_v1.1, Na_v1.3, and Na_v1.9 mRNAs were also detected while isoforms Na_v1.2, Na_v1.4, Na_v1.5,

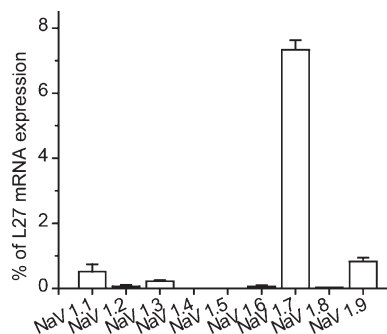


Figure 2. Quantitative RT-PCR for the indicated Na_v1.x genes from CAD cells. mRNAs for Na⁺ channel isoforms Na_v1.1, 1.3, 1.7, and 1.9 were detected from CAD cells. Data are expressed as percent of L27 mRNA (a ribosomal internal control gene) ± SEM (*n* = 6 for each).

Table 2. Primers Used for Amplification of Na_v1.1-9 Isoforms from CAD Cells

gene	primer sequence (forward–reverse)
L27	GGTCATCGTGAAGAACATTG–CATGGCAGCTGTCACTTTC
Na _v 1.1	AGAGGGAAGTTGGGATTGATG–TGGTGATTTGGAACAGGCAG
Na _v 1.2	GTTTTCCT CTCCACACCAGTC–AACCAATATCCTTCACCCGAC
Na _v 1.3	ACCAGAGCAAATACATGACCC–CAAAGTCAAAGATGTTCCAGCC
Na _v 1.4	GATGGTGCTGAAGTTGATTGC–AAAGAACGGAGCACTGATAGG
Na _v 1.5	ACATGACAGCCGAGTTTGTAG–GTCGAAGATATTCCAGCCCTG
Na _v 1.6	ATTGGCTGGAACATCTTTGA–ATCGGATGACGCGGAATA
Na _v 1.7	GAGAGCGGAGAGATGGATTTC–GCTTCAGTGGTTGTGATG
Na _v 1.8	GACATCTTCATGACGGAAGGA–ACACGAAGCCCTGGTACTTA
Na _v 1.9	TAGGAACCAAGAAGCCTCAA–AATGATGACGTCAAAGACCTG

and Na_v1.8 were either at very low or undetectable levels. Due to lack of available antibodies against the various isoforms, we were unable to determine the relative contribution of the various proteins to the Na⁺ currents in these cells. However, consistent with previous findings, in preliminary recordings, we observed that almost all of the current was blocked with 500 nM tetrodotoxin, suggesting that most of the Na⁺ current is likely contributed by Na_v1.7, Na_v1.1, and Na_v1.3 (data not shown).

In the initial set of experiments, the ability of 100 μM (*R*)-1, (*S*)-1, and lacosamide derivatives to inhibit peak inward Na⁺ currents was tested by holding CAD cells at –80 mV and running a current–voltage (*I*–*V*) protocol, which consisted of 15 ms step depolarizations ranging from –70 to +80 mV (in +10 mV increments) (Figure 3A, inset). Figure 3A shows an *I*–*V* family of Na⁺ currents recorded from CAD cells treated with 0.1% dimethyl sulfoxide (DMSO) (predrug control), 100 μM (*R*)-5, or 100 μM (*S*)-5. The transient inward current in CAD cells activated between –40 and –30 mV and reached its peak at 0 to +10 mV (Figure 3B). Peak inward Na⁺ currents elicited at each step were plotted with respect to voltage. The peak currents were normalized by cell capacitance and expressed as peak current density (pA/pF) to account for variations in cell size. CAD cells treated with 0.1% DMSO (vehicle) exhibited a peak current density of -43.7 ± 6.7 pA/pF ($n = 28$). (*R*)-1 reduced the peak current by 40%, similar to our recently published findings (46), while the inactive enantiomer (*S*)-1 exhibited no inhibition (Figure 3C).

Lacosamide derivatives (*R*)-5 and (*R*)-8 reduced peak Na⁺ currents by almost 95%, while (*R*)-6 reduced currents by about 40%, similar to (*R*)-1. While (*S*)-8 had no effect on peak Na⁺ currents, the inactive enantiomer (*S*)-5 also inhibited peak currents elicited from a holding potential of –80 mV by about 60%. Inhibition of Na⁺ currents was not accompanied by changes in reversal potential, half-maximal activation, or slope parameters (see Figure 6) for any of the lacosamide derivatives.

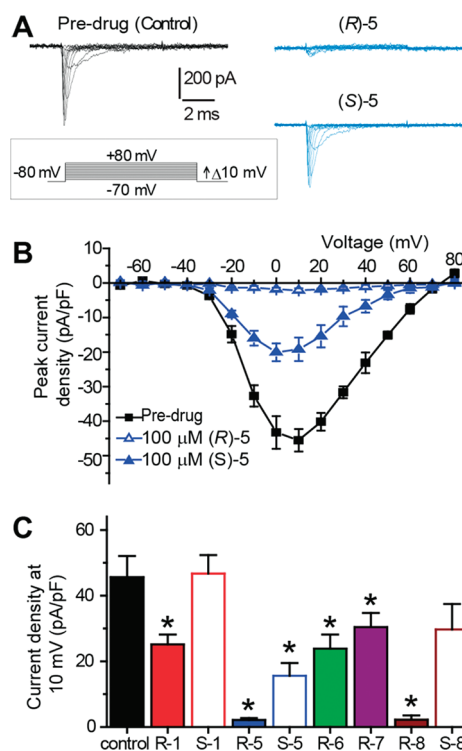


Figure 3. Inhibition of Na⁺ currents by lacosamide derivatives. (A) Representative families of current responses of CAD cells treated with 0.1% DMSO control (predrug), 100 μM (*R*)-5, or 100 μM (*S*)-5. The voltage protocol used to evoke the Na⁺ currents is shown in the boxed inset. (B) Summary of current–voltage (*I*–*V*) relationships for CAD cells treated with the compounds illustrated in (A) ($n = 8$ each). (C) Peak current density (pA/pF) measured at 0 mV for CAD cells treated with control ($n = 9$) or all lacosamide derivatives (100 μM each; $n > 7$ for each condition). *, $p < 0.05$ versus control or the respective (*S*)-isomer.

Lacosamide Derivatives Affect the Transition to a Slow Inactivated State of Na⁺ Currents in CAD Cells

(*R*)-1 has been demonstrated to reduce VGSC availability by selectively enhancing the transition to a slow-inactivated state of VGSCs (21, 22, 46). Therefore, we tested the ability of lacosamide derivatives to modulate transition to a slow-inactivated state in CAD cells. CAD

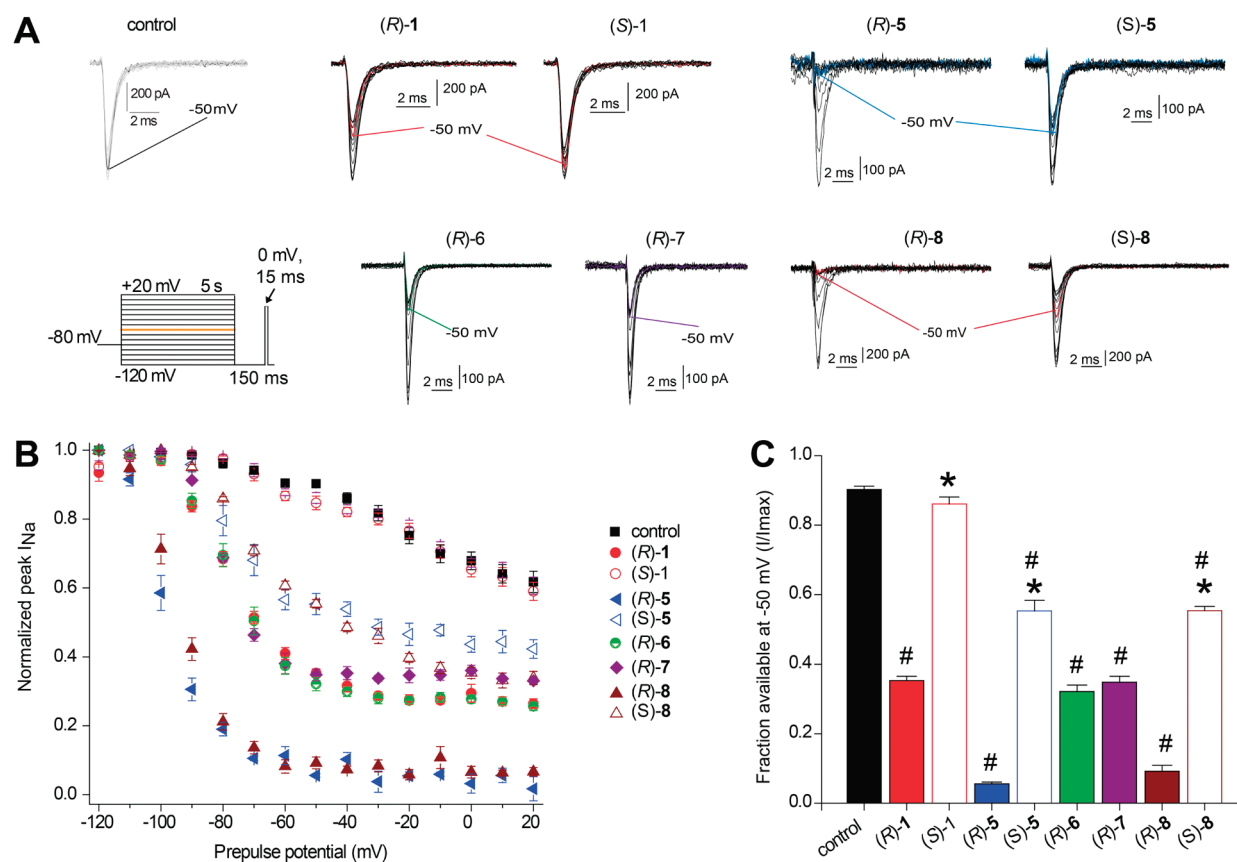


Figure 4. Enantioselective effect of steady-state slow inactivation state of Na^+ currents in CAD cells by lacosamide, lacosamide AB, and lacosamide AB&CR compounds. (A) Currents were evoked by 5 s prepulses between -120 and $+20$ mV, and then fast-inactivated channels were allowed to recover for 150 ms at a hyperpolarized pulse to -120 mV. The fraction of channels available at 0 mV was analyzed. Representative current traces from CAD cells in the absence (control, 0.1% DMSO) or presence of 100 μM of compounds as indicated. The black (control) and color (all others) traces in each panel represent the current at -50 mV (also highlighted in the voltage protocol). (B) Summary of steady-state slow activation curves for CAD cells treated with DMSO (control) or 100 μM of the indicated compounds. Drug-induced slow inactivation was most prominent in CAD cells treated with (R)-5 and (R)-8 compounds. (C) Summary of the fraction of current available at -50 mV for CAD cells in the absence or presence of (R)- or (S)-enantiomers of the indicated compounds. Asterisks (*) indicate statistically significant differences in fraction of current available between (R)- and (S)-compounds ($p < 0.05$, Student's t test). Hash marks (#) indicate a statistically significant difference in fraction of current available between control and all other conditions tested ($p < 0.05$, Student's t test). Data are from 7–12 cells per condition.

cells were held at -80 mV and conditioned to potentials ranging from -120 to $+20$ mV (in $+10$ mV increments) for 5 s. Then fast-inactivated channels were allowed to recover for 150 ms at a hyperpolarized pulse to -120 mV, and the fraction of channels available was tested by a single depolarizing pulse, to 0 mV, for 15 ms (Figure 4A, inset). The brief hyperpolarization was used to allow the channels to recover from fast inactivation while limiting recovery from slow inactivation.

A representative family of slow inactivation traces from CAD cells treated with 0.1% DMSO or 100 μM (R)-1, (R)-5–(R)-8, (S)-1, (S)-5, and (S)-8 are shown in Figure 4A. For comparison, representative current traces at -50 mV are highlighted. This potential (-50 mV) was chosen for three reasons: (1) a majority of channels are undergoing steady-state inactivation, which involves contributions from slow and fast inactivating pathways (47, 48) where -50 mV is within the steep

voltage-dependence range for each, (2) it is near the resting membrane potential (RMP) and approaching the action potential firing threshold for CNS neurons (49), where slow inactivation appears to be physiologically relevant during prolonged subthreshold depolarizations (50), and (3) changes in the Na^+ channel availability near -50 mV can impact the overlap of Na^+ current activating and inactivating under steady-state conditions (48, 51). Adding 100 μM (R)-1 to CAD cells significantly decreased the fraction of current available compared with cells without (R)-1. (S)-1 did not reduce the available current (compare -50 mV traces in all families). At -50 mV, 0.35 ± 0.01 fractional units ($n = 9$) of the Na^+ current were available, suggesting a large fraction (i.e., 0.65 ± 0.08 ; calculated as 1 minus the normalized I_{Na}) of the channels transitioned to a nonconducting (slow-inactivated) state in (R)-1-treated cells (Figure 3B, C). These findings are consistent with

earlier results that showed that (*R*)-**1**, but not (*S*)-**1**, modulated Na⁺ channel slow inactivation in neuroblastoma cells(21) and that (*R*)-**1** promoted slow inactivation in recombinant hNa_v1.7 channels expressed in HEK cells (22). The similarity of our data with these earlier findings supported our use of CAD cells to elucidate the effects of the lacosamide derivatives on Na⁺ channel function.

Using this patch-clamp protocol, physiological slow inactivation was observed at potentials more depolarized than -100 mV for (*R*)-**5** and (*R*)-**8** or at potentials more depolarized than -80 mV for (*R*)-**1** and (*R*)-**6** (Figure 4B). Compared with (*R*)-**1**, both (*R*)-**5** and (*R*)-**8** caused a significant increase in the maximal fraction of current unavailable by depolarization (20 mV; control, 0.62 ± 0.03 , $n = 8$; (*R*)-**1**, 0.26 ± 0.01 , $n = 9$; (*R*)-**5**, 0.02 ± 0.03 , $n = 8$; (*R*)-**8**, 0.07 ± 0.01 , $n = 9$; $p < 0.01$, Mann–Whitney U test). Almost all (0.95 ± 0.01 ; $n = 8$) channels of (*R*)-**5**-treated cells were in a slow-inactivated state, while only 0.35 ± 0.09 ($n = 8$) of its stereoisomer (*S*)-**5** Na⁺ channels were. (*R*)-**8** also had a similar enantioselective effect to the (*S*)-**8** stereoisomer, with 0.90 ± 0.02 ($n = 8$) and 0.45 ± 0.08 ($n = 9$) of the channels in a slow-inactivated state, respectively. Both (*R*)-**6** and (*R*)-**7** had slow-inactivated fractions similar to (*R*)-**1**: 0.68 ± 0.07 ($n = 8$) and 0.66 ± 0.05 ($n = 8$).

To better understand the interaction among lacosamide derivatives and the extent to which they induce slow inactivation, we performed concentration response curves for slow inactivation induction for each compound. An example of the concentration response for slow inactivation induced by 0.1–100 μM (*R*)-**5** is shown in Figure 5A. Fits of the concentration response of slow inactivation against the $V_{1/2}$ of slow inactivation provide a 50% inhibitory concentration (IC₅₀) value of 8.1 μM (Figure 5B). Table 1 shows the IC₅₀ values for slow inactivation induced by the other lacosamide derivatives. Compared with the IC₅₀ value of 85 μM estimated for the slow inactivation induced by (*R*)-**1**, the IC₅₀ value for (*R*)-**7** was 7.1-fold lower while (*R*)-**8** was 5.3-fold lower. In all cases, the IC₅₀ value for slow inactivation was lower for the (*R*)-stereoisomer versus the (*S*)-enantiomer.

Collectively, these data indicate that lacosamide derivatives (*R*)-**5**–(*R*)-**8** are more effective at inducing the transition of Na⁺ channels to a slow-inactivated state than the parent (*R*)-**1**, and lacosamide compounds (*R*)-**1**, (*R*)-**5**, and (*R*)-**8** modulate Na⁺ channel slow inactivation in an enantioselective fashion. While the enhanced activity (lower IC₅₀ values) observed for the (*R*)-**2** (i.e., (*R*)-**8**) and the (*R*)-**4** (i.e., (*R*)-**5**–(*R*)-**7**) derivatives compared with (*R*)-**1** is significant, we are uncertain to attribute specific structural and physiochemical properties (e.g., size, lipophilicity) to the decreased IC₅₀ values for the lacosamide AB and AB&CR agents. Nonetheless, the

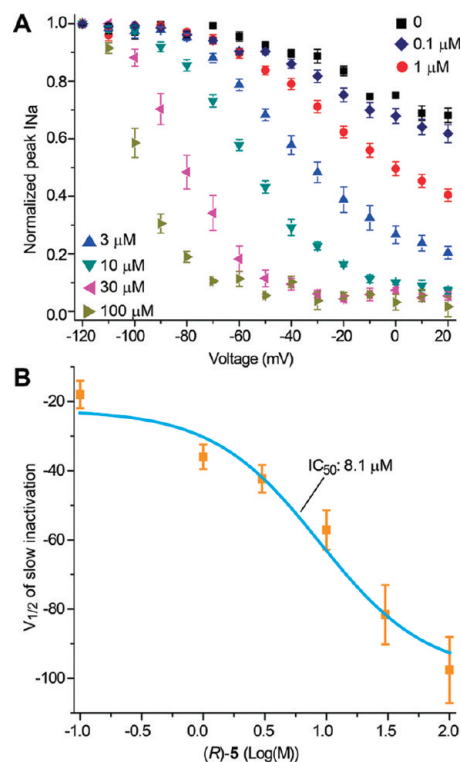


Figure 5. Concentration response curve for (*R*)-**5** on the induction of Na⁺ currents slow inactivation. (A) Summary of steady-state slow activation curves for CAD cells treated with DMSO (0) or 0.1–100 μM (*R*)-**5**. Each curve was fit with a Boltzmann equation to yield values for $V_{1/2}$, the voltage of half-maximal inactivation. (B) Concentration versus $V_{1/2}$ response curve for effects on slow inactivation. To estimate the half-maximal value for induction of slow inactivation, dose–response curves were fit using the equation: $Y = A_1 + (A_2 - A_1)/(1 + 10^{(\log X_0 - x)p})$, where Y is the measured response of the I_{Na} , A_2 and A_1 are the maximum and minimum responses, respectively, of the I_{Na} obtained with a control sample, p is the slope parameter of the dose–response curve, x is the applied dose, and $\log X_0$ is the center of the curve that is the concentration for half the I_{Na} response. The curves were well-fitted with this dose–response function ($R^2 > 0.91$). Each point is the mean \pm SEM of 6–9 CAD cell recordings. The half-maximal values for slow inactivation for the rest of the compounds are shown in Table 1.

calculated log P values (ACDLabs software) for the (*R*)-**2** and (*R*)-**4** derivatives (1.14–2.42) were higher than that for (*R*)-**1** (0.73), suggesting that these agents are more lipophilic than (*R*)-**1** and are therefore likely to achieve higher intracellular concentrations under the conditions we are using. It is also possible that these structural modifications increase the interaction between lacosamide derivatives and their receptor(s). The much lower IC₅₀ values observed for (*R*)-**2** and the (*R*)-**4** derivatives compared with (*R*)-**1** might be due to a combination of these effects.

Activation Properties of Na⁺ Currents in CAD Cells Are Not Affected by Lacosamide Derivatives

Because changes in current amplitudes could result from changes in channel gating (52), we tested if lacosamide

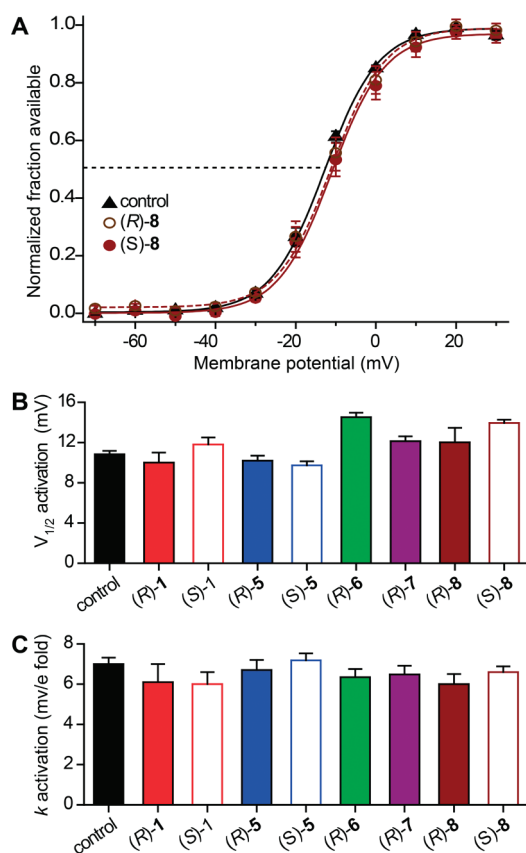


Figure 6. Activation properties of Na^+ currents are not affected by lacosamide, lacosamide AB, and lacosamide AB&CR compounds in CAD cells. Values for $V_{1/2}$, the voltage of half-maximal activation, and the slope factors (k) were derived from Boltzmann distribution fits to the individual recordings and averaged to determine the mean (\pm SEM) voltage dependence of activation. The voltage protocol used to evoke current responses is shown in Figure 2A. Representative Boltzmann fits for DMSO, 100 μM (R)-8, and 100 μM (S)-8 are shown (A). The $V_{1/2}$ (B) and k (C) of activation were not different among any of the compounds tested ($p > 0.05$, one-way ANOVA). Data are from 7–12 cells per condition.

derivatives altered the voltage-dependent activation properties of Na^+ currents in CAD cells. Changes in activation for the CAD cells treated with the derivatives were measured by whole-cell ionic conductances by comparing their respective midpoints ($V_{1/2}$) and slope factors (k) in response to changes in command voltage (Figure 6A). An analysis of all $V_{1/2}$ (Figure 6B) and k (Figure 6C) values showed that there were no changes in the steady-state activation properties of Na^+ currents between CAD cells treated with DMSO control or with any of the lacosamide derivatives. These data indicate that lacosamide derivatives do not affect the channel's transition from a closed to an open conformation.

Fast Inactivation Properties of Na^+ Currents in CAD Cells Are Not Affected by Lacosamide Derivatives

Our data indicated that (R)-1 and lacosamide derivatives (R)-5–(R)-8 exhibit preferential effects on the

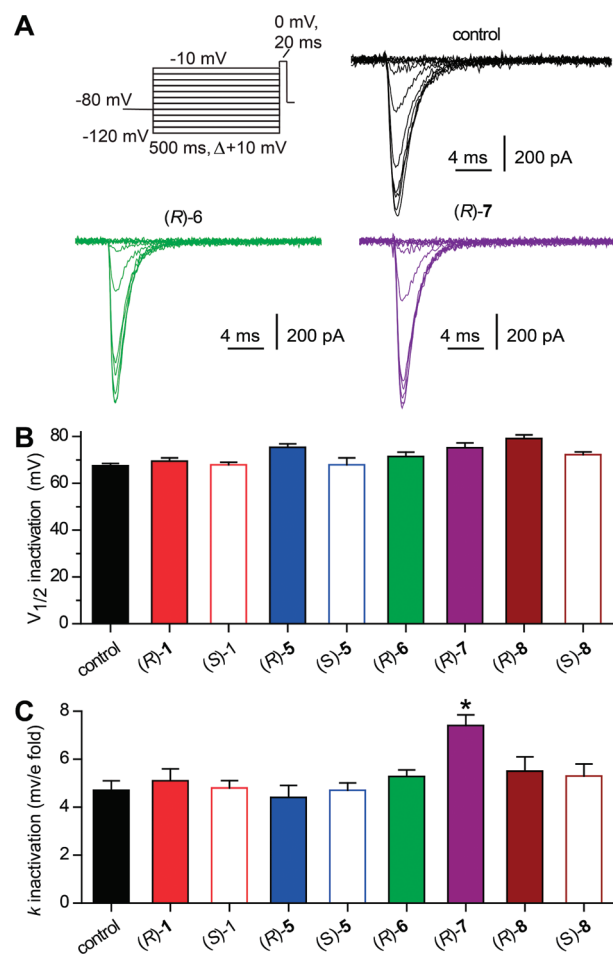


Figure 7. Fast inactivation properties of Na^+ currents are not affected by lacosamide, lacosamide AB, and lacosamide AB&CR compounds in CAD cells. (A) Voltage protocol for fast inactivation. Representative current traces showing voltage-dependent fast inactivation of Na^+ currents from CAD cells treated with 0.1% DMSO control (black traces), 100 μM (R)-6 (green traces), or 100 μM (R)-7 (purple traces). Values for $V_{1/2}$, the voltage of half-maximal inactivation, and the slope factors (k) were derived from Boltzmann distribution fits to the individual recordings and averaged to determine the mean (\pm SEM) voltage dependence of steady-state inactivation. The $V_{1/2}$ (B) and k (C) of steady-state fast inactivation were not different among any of the conditions tested ($p > 0.05$, one-way ANOVA), with the exception of the k of (R)-7, which was significantly different from all other conditions ($p < 0.05$, one-way ANOVA).

slow inactivated state of Na^+ channels. We asked if (R)-1 and its derivatives could enhance steady-state fast inactivation. For this, we used a protocol (see Figure 7) designed to accumulate channels in a fast-inactivated state, as previously described (28). Cells were held at -80 mV, stepped to inactivating prepulse potentials ranging from -120 to -10 mV (in 10 mV increments) for 500 ms, and then the cells were stepped to 0 mV for 20 ms to measure the available current. A 500 ms conditioning pulse was used because it allows all of the endogenous channels to transition to a fast-inactivated state at all potentials

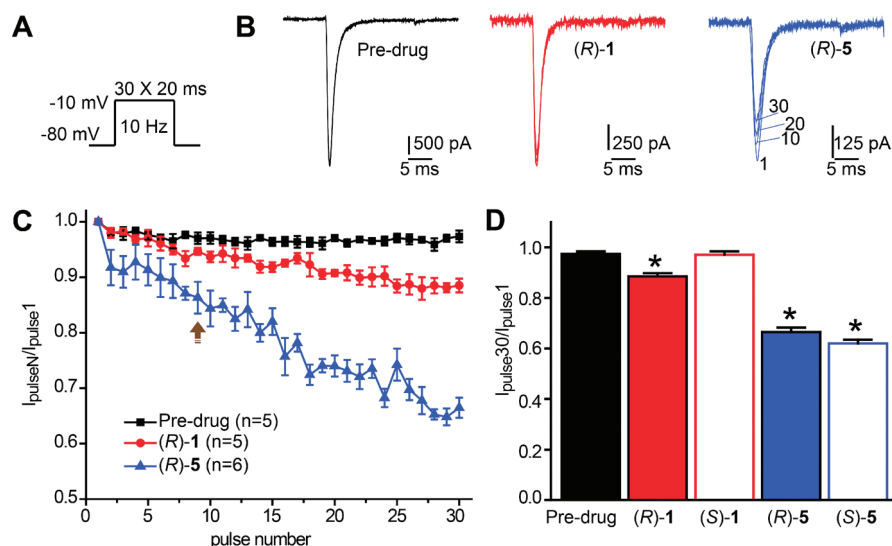


Figure 8. Effects of frequency-dependent block by lacosamide and the isothiocyanate lacosamide AB agent (*R*)-5 on Na⁺ currents in CAD cells. (A) The frequency dependence of block was examined by holding cells at a hyperpolarized potential of -80 mV and evoking currents at 10 Hz by 20 ms test pulses to -10 mV. (B) Representative overlaid traces are illustrated of the 1st, 10th, 20th, and 30th pulses for control (pre-drug) and in the presence of (*R*)-1 ($100 \mu\text{M}$) and (*R*)-5 ($15 \mu\text{M}$). (C) Plot summarizing the average frequency-dependent decrease in current amplitude (\pm SEM) produced by (*R*)-1 and (*R*)-5 but not by control conditions (for clarity the use-dependence of the (*S*)-enantiomers is not shown). (D) Summary of the maximal decrement in current amplitude observed at the end of the 30 pulse train for control, (*R*)-1, (*S*)-1, (*R*)-5, and (*S*)-5. (*R*)-1, (*R*)-5, and (*S*)-5 caused a significant decrease in current amplitude compared with pretreatment (*, $p < 0.05$, one-way ANOVA with Dunnett's posthoc test). Note the rapid frequency-dependent facilitation of block by (*R*)-5 that was observed beginning as early as pulse 8 (arrow). Data are from 5–6 cells per condition.

assayed. To negate any possible effects of time-dependent shifts in the voltage dependence of fast inactivation, comparisons were made on data obtained 3–4 min after establishing the whole-cell recording configuration from cells in the absence of drug with similar data obtained in the presence of the lacosamide derivatives. Steady-state, fast inactivation curves of Na⁺ currents from DMSO-, (*R*)-1-, (*S*)-1-, (*R*)-5–(*R*)-8-, (*S*)-5-, and (*S*)-8-treated CAD cells were well fitted with a single Boltzmann function ($R^2 > 0.9987$ for all conditions). The $V_{1/2}$ value for inactivation for 0.1% DMSO-treated cells was -67.5 ± 1.0 mV ($n = 8$), which was not different from that of (*R*)-1-treated cells (-69.5 ± 1.3 mV; $n = 9$; $p > 0.05$; see Figure 7B). No statistically significant shifts in the voltage-dependence of fast inactivation were observed for any of the (*R*)-5–(*R*)-8 or (*S*)-5 and (*S*)-8 compounds (see Figure 7B). Neither were the slopes (k) of the fast inactivation curves affected by lacosamide derivatives (see Figure 7C), with the exception of (*R*)-7, which had a slope that was about 55% shallower than that of cells treated with DMSO ($p < 0.05$, see Figure 7C).

Frequency-Dependent Block of Na⁺ Currents by Lacosamide and AB Agent (*R*)-5 on CAD Cells

We selected (*R*)-1, (*S*)-1, (*R*)-5, and (*S*)-5 to study the frequency-dependent block (and development of inhibition/slow inactivation; see next section) of Na⁺ currents by lacosamide and lacosamide analogues. (*R*)-1 and

(*S*)-1, its inactive isomer, served as controls, while (*R*)-5 is the most active lacosamide agent we evaluated in this study and (*S*)-5 is its corresponding isomer. Block of Na⁺ currents in an activity- or use-dependent manner is a useful property for antiepileptic drugs, since it allows for preferential decreases in Na⁺ channel availability during high-frequency (i.e., seizures) but not low-frequency firing. Thus, we next tested if (*R*)-1 ($100 \mu\text{M}$), (*S*)-1 ($100 \mu\text{M}$), (*R*)-5 ($15 \mu\text{M}$), and (*S*)-5 ($100 \mu\text{M}$) could elicit use-dependent block. A train of 30 test pulses (20 ms to -10 mV) was delivered from a holding potential of -80 mV at 10 Hz. The available current in control and in the presence of drug agents was calculated by dividing the peak current at any given pulse (pulse_N) by the peak current in response to the initial pulse (pulse₁). Both (*R*)-1 and (*R*)-5 reduced current amplitude compared with control (Figure 8C). Block was also observed with (*S*)-5; this was likely due to the high ($100 \mu\text{M}$) concentration used. In contrast, (*S*)-1 did not elicit any use-dependence block at the concentration tested. While use-dependent block by (*R*)-1 was first observed by about the 19th pulse in the train, (*R*)-5 did not show such latency with rapid block seen as early as pulse 8 (Figure 8C, arrow). By the last pulse, compared to control, the peak current was $\sim 10\%$ lower in the presence of (*R*)-1 and 30% lower in the presence of (*R*)-5 (Figure 8C). The isothiocyanate lacosamide AB agent (*R*)-5, despite being used at $15 \mu\text{M}$ in these experiments, was about

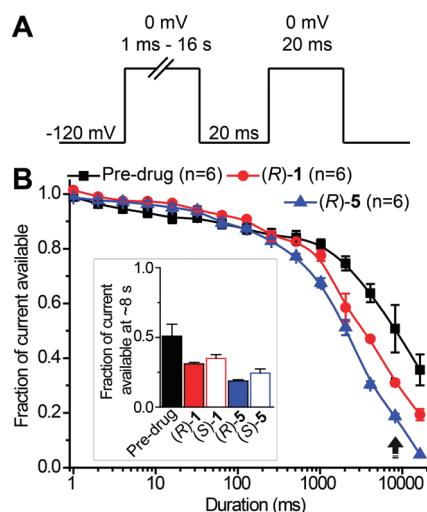


Figure 9. Rate of development of inhibition/slow inactivation is altered by lacosamide and the isothiocyanate lacosamide AB agent (*R*)-5 in CAD cells. (A) Voltage protocol for development of inhibition/slow inactivation. Following a variable conditioning pulse to 0 mV, a 20 ms pulse to -120 mV allows recovery from fast inactivation (but not block) before the fraction of current available with the 20-ms pulse to 0 mV. (B) (*R*)-1 increased the rate of development of inactivation/inhibition compared to that observed in vehicle-treated CAD cells at prepulse durations greater than 2 s. For (*R*)-5, this increase occurred at prepulse durations longer than 512 ms ($p < 0.05$, one-way ANOVA with Dunnett's postdoc test). Inset: The fraction of current available at 8 s (arrow) prepulse duration was significantly smaller for (*R*)-5 (0.18 ± 0.009 , $n = 6$), (*R*)-1 (0.31 ± 0.01 , $n = 6$), its inactive isomer (*S*)-1 (0.35 ± 0.03 , $n = 6$), and (*S*)-5 (0.26 ± 0.08 , $n = 5$) compared to vehicle-treated cells (0.51 ± 0.08 , $n = 6$; $p < 0.05$, one-way ANOVA with Dunnett's postdoc test).

25% more effective in facilitating use-dependent block of Na^+ currents.

Rate of Development of Inhibition/Slow Inactivation Is Altered by Lacosamide and AB Agent (*R*)-5 on CAD Cells

To understand the interaction between (*R*)-1 and (*R*)-5 and Na^+ channels, we next investigated the time course of development of block by these agents and their enantiomers. Development of block was examined by holding the cells at -120 mV in the absence or presence of (*R*)-1 (100 μM), (*S*)-1 (100 μM), (*R*)-5 (15 μM), and (*S*)-1 (100 μM), prepulsing the cells to 0 mV for varying amounts of time to allow block to develop, hyperpolarizing the cells to -120 mV for 20 ms to allow unbound channels to recover from fast inactivation, then stepping the cells to 0 mV for 20 ms to determine the fraction of channels available for activation (Figure 9A). The reduction in the fraction of current available is indicative of the time course for the development of slow inactivation. The time course of reduction in channel availability without drug as well as in the presence of (*R*)-1 and (*R*)-5 was biphasic, with a fast component likely representing

development of block of fast-inactivated channels and a slow component that was consistent with the time course of development of slow inactivation (Figure 9B). The time constant for development of block was ~ 1.5 -fold faster in cells treated with (*R*)-1 (100 μM) or (*R*)-5 (15 μM) compared to vehicle-treated cells. Both (*S*)-1 and (*S*)-5 enantiomers caused a reduction in the fraction of current at 8 s (Figure 9, inset box) that trended toward a difference from the (*R*)-enantiomers but was not statistically significant. At this point, we are not sure of why stereospecificity is not observed for these drugs in this particular protocol.

Select Lacosamide Derivatives May Irreversibly Affect the Transition to a Slow-Inactivated State of Na^+ Currents in CAD Cells

If either lacosamide AB ((*R*)-4) or lacosamide AB&CR ((*R*)-2) irreversibly affects Na^+ channel slow inactivation by covalently modifying a receptor that affects this process, then slow inactivation should still be observed when the drug derivative is removed from the CAD cells by extensive washing with an extracellular bath solution. Alternatively, if either (*R*)-1, (*R*)-2, or (*R*)-4 reversibly modify Na^+ channel slow inactivation by a noncovalent interaction, then slow inactivation will be lost when the lacosamide derivative is removed by washing. To distinguish these possibilities, we compared the effects of (*R*)-1 with the electrophilic AB agent, (*R*)-5, and the photolabile AB agents, (*R*)-6 and (*R*)-7, on Na^+ channel inactivation using conditions designed to activate the AB group.

In the initial series of experiments, we determined that CAD cells treated with 0.1% DMSO (control) had about 10% (at -50 mV) of their Na^+ channels in a slow-inactivated fraction (Figures 3B, 9, and 10), a value that was not different if the cells were subsequently washed for 5 min or longer with an extracellular bath solution (data not shown). Next, we compared the extent of Na^+ channel slow inactivation induced in CAD cells upon 10 min incubation with 100 μM (*R*)-1 or 40 μM (*R*)-5 followed by a 5 min wash period with fresh extracellular bath solution. We expected that incubation of the CAD cells with (*R*)-5 at 37 $^\circ\text{C}$ for 10 min would be sufficient to lead to (some) irreversible adduction of a receptor, provided binding was modest and a nucleophile was positioned near the isothiocyanate group (23, 26). The slow inactivation curves in the absence, presence, or following washout of these agents are shown in Figure 10A, G, and Figure 10B, H illustrates the extent of slow inactivation at -50 mV under these conditions. We observed that the effect of (*R*)-1 was completely reversed following the 5 min wash, while for (*R*)-5 a small but significant fraction ($\sim 10\%$) of the channels remained in a slow-inactivated state after the CAD cells were washed. The apparent modest irreversibility in

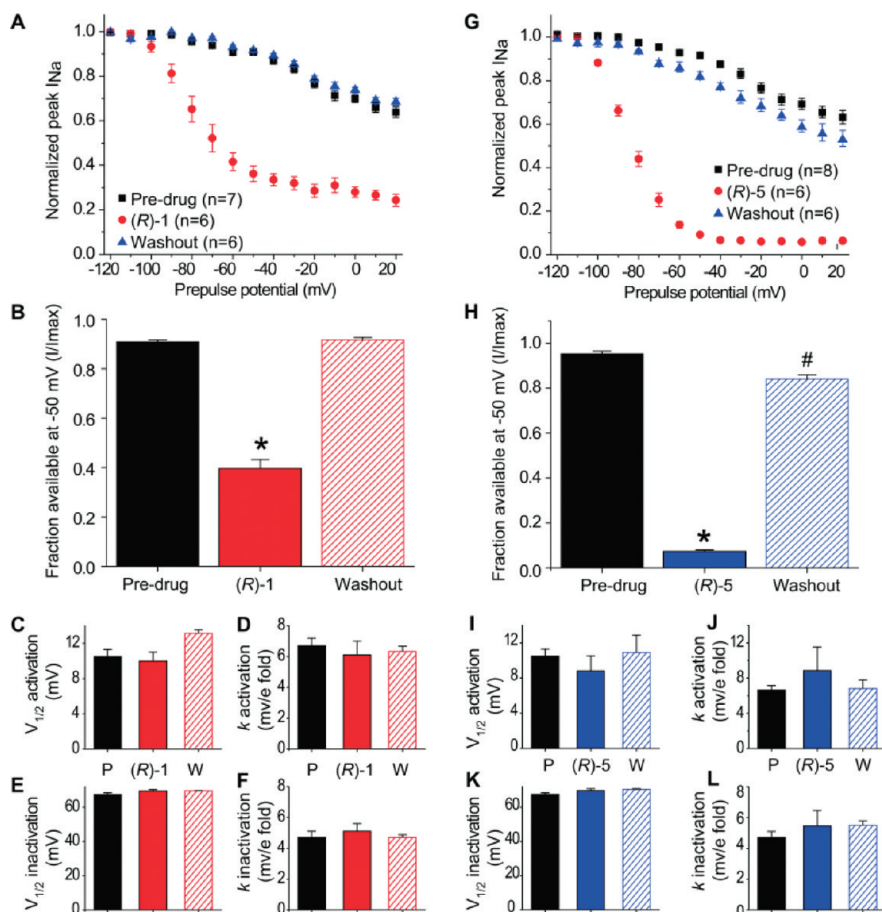


Figure 10. Effects of lacosamide and the isothiocyanate lacosamide AB agent (*R*-5) on Na⁺ currents slow inactivation in CAD cells. Summary of steady-state slow activation curves for CAD cells treated for 10 min at 37 °C with DMSO control (predrug), 100 μM (*R*-1) (A), or 40 μM (*R*-5) (G), or they were treated with 100 μM (*R*-1) (A) or 40 μM (*R*-5) (G) and washed with complete medium (see Methods) for 5 min. Currents were evoked as described in the legend to Figure 1. Numbers of cells are indicated in parentheses (*n*). (B, H) Summary of the fraction of current available at -50 mV for CAD cells in the absence or presence of the indicated drug conditions. Asterisks (*) indicate statistically significant differences in fraction of current available between either (*R*-1) or (*R*-5) and predrug values or between (*R*-1) or (*R*-5) and washout values (*p* < 0.05, Student's *t*-test). Hash marks (#, H) indicate a statistically significant difference in fraction of current available at -50 mV between predrug and washout values (*p* < 0.05, Student's *t* test). Data are from 7–12 cells per condition. The *V*_{1/2} (C, I) and *k* (D, J) of activation were not different among any of the conditions tested (*p* > 0.05, one-way ANOVA). Similarly, the *V*_{1/2} (E, K) and *k* (F, L) of steady-state fast inactivation were not different among any of the conditions tested (*p* > 0.05, one-way ANOVA).

slow inactivation for (*R*-5) was not due to any changes in steady-state activation or fast inactivation, as these values were not different in predrug, drug, or washout conditions (Figure 10I–L). However, we observed no appreciable changes in the current amplitudes after the CAD cells were washed. The current amplitudes at -10 mV, a voltage at which Na⁺ channel activation is linear and slow inactivation has reached steady state, recovered by 74% and 72% for (*R*-1) and (*R*-5), respectively, compared with predrug values. Thus, the data only suggest that (*R*-5) modified the receptor(s) responsible for Na⁺ channel slow inactivation.

Since the photolabile agents, (*R*-6) and (*R*-7), were better modulators of Na⁺ channel slow inactivation than (*R*-1), we next tested their effects in CAD cells upon activation. Accordingly, the CAD cells containing (*R*-6) were irradiated with ultraviolet light (312 nm) for 5 min

using a hand-held UV transilluminator (26). The fraction of channels in the slow-inactivated state was similar in cells exposed to DMSO control (predrug) and UV alone treatments (Figure 11A–C). For the (*R*-6) UV-treated cells, ~45% of the channels had transitioned to a slow-inactivated state, a value that was not significantly different from the 50% of channels in the slow-inactivated state in nonirradiated cells exposed to (*R*-6) (Figure 11A–C). Importantly, for cells treated with (*R*-6), exposed to UV irradiation and then washed for 5 min, about 20% of Na⁺ channels remained in a slow-inactivated state compared with ~10% of channels in the slow-inactivated state in cells exposed to UV irradiation alone (Figure 11B, C). This increase in the percentage of Na⁺ channels in the slow-inactivated state may indicate that a small fraction of the receptors responsible for this phenomenon have been covalently adducted by

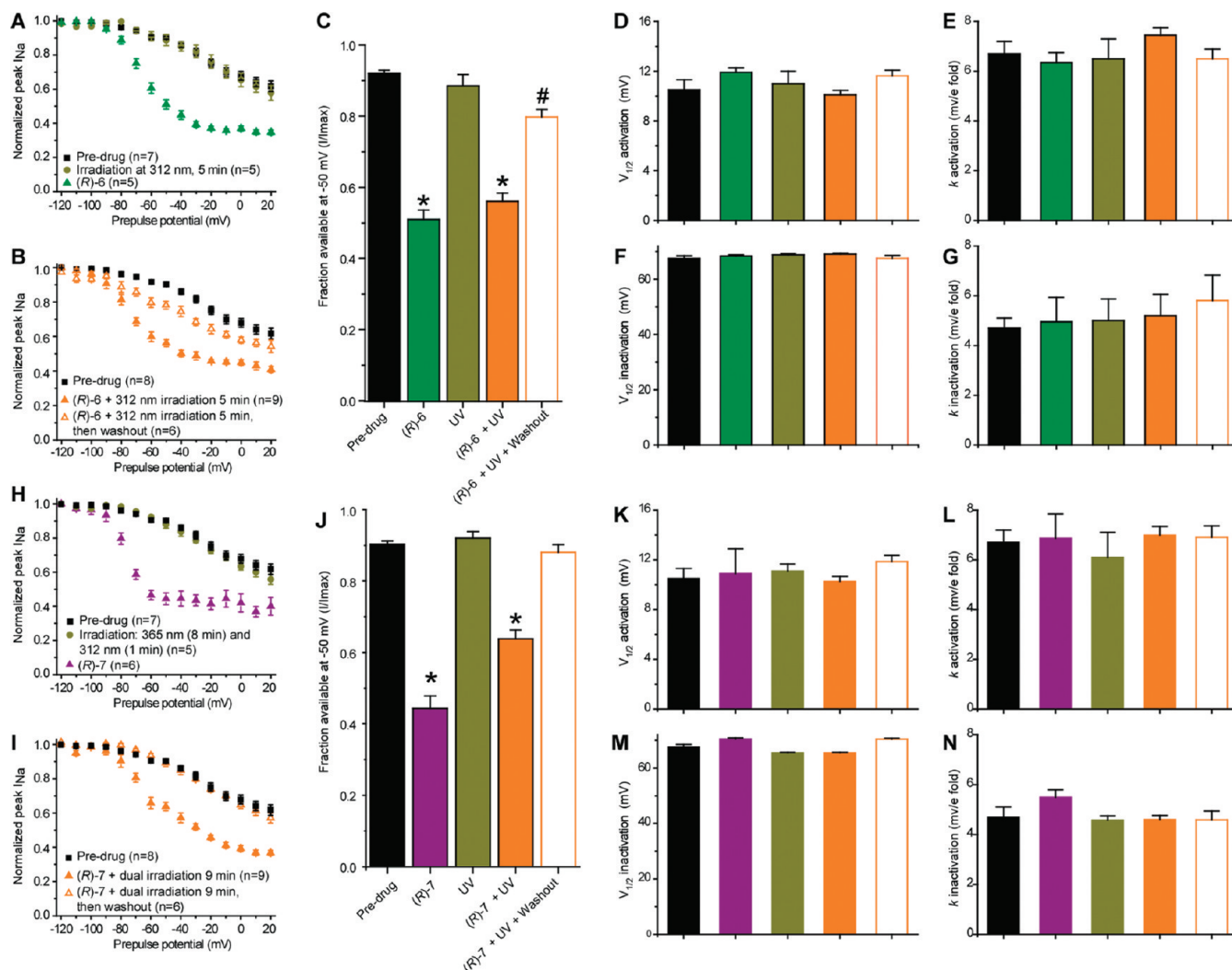


Figure 11. Effects of the azido lacosamide AB agent (*R*-6) and 3-(trifluoromethyl)-3H-diaziriny-3-yl lacosamide AB agent (*R*-7) on Na⁺ current slow inactivation in CAD cells. Summary of steady-state slow activation curves for CAD cells treated with DMSO control (predrug), 40 μM (*R*-6) (A, B), or 30 μM (*R*-7) (H, I), or they were UV irradiated in the presence or absence of the indicated drugs. The experiments were repeated and followed by a 5 min wash with complete medium, as described in Methods. CAD cells were exposed to a photoactivation regimen of irradiation at 312 nm for 5 min (in the absence or presence of (*R*-6)) or sequential irradiation at 365 nm for 8 min followed by irradiation at 312 nm for 1 min (in the absence or presence of (*R*-7)). (C, J) Summary of the fraction of current available at -50 mV for CAD cells in the absence or presence of the indicated drug and UV conditions. Asterisks (*) indicate statistically significant differences in fraction of current available between (*R*)-AB and predrug, UV, or (*R*)-AB + UV + washout values ($p < 0.05$, Student's t test). Hash marks (#) indicate a statistically significant difference in fraction of current available at -50 mV between predrug and washout values or between UV and (*R*) + UV + washout values ($p < 0.05$, Student's t test). Data are from 7–12 cells per condition. The $V_{1/2}$ (D, K) and k (E, L) of activation were not different among any of the conditions tested ($p > 0.05$, one-way ANOVA). Similarly, the $V_{1/2}$ (F, M) and k (G, N) of steady-state fast inactivation were not different among any of the conditions tested ($p > 0.05$, one-way ANOVA).

photoactivated (*R*-6). The current amplitudes at -10 mV recovered by 79% in cells treated with (*R*-6), exposed to UV irradiation, and then washed for 5 min compared with predrug values, and by 75% compared with the UV-treated cells that had not been treated with (*R*-6). There were no changes in steady-state activation or fast inactivation between any of the conditions tested (Figure 11D–G).

Photoactivation of (*R*-7) in CAD cells was achieved by exposing (*R*-7)-treated cells to sequential irradiation at 365 nm for 8 min followed by 312 nm for 1 min (53).

The fraction of channels in the slow-inactivated state were similar in cells exposed to DMSO control (predrug) and UV irradiation alone treatments. When the cells were treated with (*R*-7) and then photoactivated, about 35% of Na⁺ channels were observed to accumulate in the slow-inactivated state compared with 65% in (*R*-7)-treated cells without light (Figure 11I, J). We tentatively attribute the loss of (*R*-7) activity to the photodegradation of the (trifluoromethyl)diazirine moiety leading to an inactive agent. In cells treated with (*R*-7), exposed to UV irradiation, and then washed for 5 min, about 10%

of Na⁺ channels remained in a slow-inactivated state, a value nearly identical to that observed in cells exposed to DMSO control or UV alone. This finding suggests that photoactivation of (*R*)-7 did not lead to irreversible receptor adduction. The current amplitudes at -10 mV in cells treated with (*R*)-7, exposed to UV irradiation, and then washed for 5 min recovered by 87% compared with the values in cells exposed to DMSO control or UV alone. There were no changes in steady-state activation or fast inactivation in any of the conditions tested (Figure 11D–G).

Conclusions

The data validated that incorporating the selected AB and the CR groups in (*R*)-1 did not affect the ability of these agents to induce Na⁺ slow inactivation processes in CAD cells. Remarkably, we found that both (*R*)-2 and (*R*)-4 agents were more effective than (*R*)-1 in promoting Na⁺ channel slow inactivation. This finding may reflect that the lacosamide agents bind tighter to the receptor(s) responsible for slow inactivation or is simply a manifestation of their higher intracellular concentrations. In this regard, incorporating AB and CR units within the (*R*)-1 likely increases the lipophilicity of these compounds over (*R*)-1 and perhaps increases their entry into the cell. Finally, we obtained preliminary evidence for modest permanent Na⁺ channel slow inactivation upon treatment with either the electrophilic AB agent (*R*)-5 or the photolabile AB (*R*)-6 after AB activation. Our study did not allow us to address how (*R*)-1, (*R*)-2, and (*R*)-4 affect Na⁺ channel slow inactivation. The precise pathway for (*R*)-1 modulation of Na⁺ channels has not been revealed (21, 22). Thus, one possibility is that (*R*)-1, (*R*)-2, and (*R*)-4 bind to a segment of the Na⁺ channel promoting slow-inactivation. Alternatively, (*R*)-1 and its derivatives may bind to another receptor(s) in CAD cells that affects Na⁺ slow inactivation. These questions remain central to our ongoing studies. We expect that (*R*)-5, (*R*)-6, and (*R*)-8, as well as second generation lacosamide AB and AB&CR agents that provide higher levels of permanent Na⁺ channel slow inactivation, may permit us to distinguish these and other pathways.

Methods

Chemistry

Preparation of 4-[3-(Trifluoromethyl)-3H-diazirin-3-yl]-benzenemethanamine (10). Triphenylphosphine polymer bound (Fluka, cat # 93094) (1.6 g/mol, 6.3 mmol) was added to an aqueous (378 μL, 21.0 mmol)/THF (10 mL) solution of 3-[4-(azidomethyl)phenyl]-3-(trifluoromethyl)-3H-diazirine (37) (11) (506 mg, 2.1 mmol). The mixture was shaken until the starting material was no longer evident by TLC analysis (18 h). The triphenylphosphine-based support was filtered and washed with CH₂Cl₂, and the filtrate was concentrated

in vacuo to obtain 350 mg (80%) of a yellow oil corresponding to the free amine: ¹H NMR (CDCl₃) δ 1.35–1.50 (br s, NH₂), 3.89 (s, CH₂), 7.17 (d, *J* = 8.2 Hz, 2 ArH), 7.35 (d, *J* = 8.2 Hz, 2 ArH); ¹³C NMR (CDCl₃) δ 28.4 (q, *J* = 39.9 Hz, C diazirine), 45.9 (CH₂NH₂), 122.2 (q, *J* = 273.2 Hz, CF₃), 126.7, 127.5, 145.0 (4 ArC), one signal was not detected and is believed to overlap with nearby peaks; HRMS (*M* + *H*⁺) (ESI⁺) 216.0747 [*M* + *H*⁺] (calcd for C₉H₈F₃N₃H⁺ 216.0749). The amine was stored and used as the hydrochloride salt.

Preparation of (*R*)-*N*-(4-(3-(Trifluoromethyl)-3H-diazirin-3-yl)benzyl)-2-Acetamido-3-methoxypropionamide ((*R*)-7). 4-[3-(Trifluoromethyl)-3H-diazirin-3-yl]-benzenemethanamine hydrochloride (10·HCl) (933 mg, 3.7 mmol) was added to a THF (31 mL) solution of the (*R*)-2-acetamido-3-methoxypropionic acid(36) ((*R*)-9) (500 mg, 3.1 mmol), and the mixture was stirred at room temperature (5 min) and then NMM (0.41 mL, 3.7 mmol) was added. The mixture was stirred a room temperature (5 min), DMTMM (1.03 g, 3.7 mmol) was added, and the mixture was again stirred at room temperature (16 h). The white precipitate was filtered, and the filtrate was concentrated in vacuo. The residue was purified by flash column chromatography on silica gel with EtOAc/acetone (10/0 to 6/4) as the eluant to obtain a white solid (810 mg, 73%): *R*_f = 0.74 (EtOAc); mp 195 °C (decomp); [α]_D²⁵ -11.0° (*c* 0.5, CHCl₃); IR (nujol) 3278, 1635, 1554, 1458, 1375, 1236, 1186, 1148, 1054, 940, 805, 731 cm⁻¹; ¹H NMR (CDCl₃) δ 2.02 (s, CH₃C(O)), 3.38 (s, OCH₃), 3.44 (dd, *J* = 7.2, 9.0 Hz, CHH'), 3.80 (dd, *J* = 4.2, 9.0 Hz, CHH'), 4.40–4.51 (m, CH₂), 4.52–4.59 (m, CH), 6.45 (d, *J* = 6.0 Hz, NHC(O)CH₃), 6.89–6.98 (br t, NHCH₂), 7.15 (d, *J* = 8.2 Hz, 2 ArH), 7.29 (d, *J* = 8.2 Hz, 2 ArH), addition of excess (*R*)-(-)-mandelic acid to a CDCl₃ solution of (*R*)-7 gave only one signal for the acetyl methyl and one signal for the ether methyl protons; ¹³C NMR (CDCl₃) δ 23.2 (CH₃C(O)), 28.3 (q, *J* = 40.1 Hz, C diazirine), 43.0 (CH₂N), 52.5 (CH), 59.1 (OCH₃), 71.5 (CH₂OCH₃), 122.1 (q, *J* = 273.1 Hz, CF₃), 126.9, 127.8, 128.3, 139.9 (4 ArC), 170.2, 170.4 (2 CO); HRMS (*M* + *H*⁺) (ESI⁺) 359.1334 [*M* + Na⁺] (calcd C₁₅H₁₇F₃N₄O₃H⁺ 359.1331). Anal. Calcd. for C₁₅H₁₇F₃N₄O₃·0.05C₃H₆O: C, 50.34; H, 4.81; F, 15.83; N, 15.56. Found: C, 50.59; H, 4.76; F, 15.46; N, 15.24.

Pharmacology

Compounds were screened under the auspices of the National Institutes of Health's Anticonvulsant Screening Program. Experiments were performed in male rodents [albino Carworth Farms No. 1 mice (intraperitoneal route, ip), albino Spague-Dawley rats (oral route, po)]. Housing, handling, and feeding were in accordance with recommendations contained in the *Guide for the Care and Use of Laboratory Animals* (National Academies Press). Anticonvulsant activity was established using the MES test(24) and the scMet test (44), according to previously reported methods (16).

Catecholamine A Differentiated (CAD) Cells

CAD cells were grown at 37 °C and in 5% CO₂ (Sarstedt, Newton, NC) in Ham's F12/EMEM medium (GIBCO, Grand Island, NY), supplemented with 8% fetal bovine serum (FBS; Sigma, St. Louis, MO) and 1% penicillin/streptomycin (100% stocks, 10 000 U/mL penicillin G sodium and 10 000 μg/mL streptomycin sulfate) (45, 46). Cells were passaged every 6–7 days at a 1:25 dilution.

Quantitative Reverse Transcriptase PCR (qRT-PCR)

The mRNA levels of genes were quantitatively evaluated by real-time qRT-PCR as described (54). Single-stranded cDNA was synthesized from CAD cell RNA using reverse transcriptase (Bioline) with oligo-dT primers. For qRT-PCR, resultant cDNA samples were amplified on an ABI PRISM 7900HT Sequence Detection system (Applied Biosystems) using SYBR Green as a reporter. In most cases, the PCR reaction was run under the following conditions: 1×, 50 °C, 2 min; 1×, 95 °C, 10 min; 45×, 95 °C, 15 s, 60 °C, 1 min; 1×, 72 °C, hold. To check whether amplification yielded PCR products with a single molecular weight, the PCR products were electrophoresed and sequenced. In addition, melting curve analysis was performed to confirm the authenticity of the PCR products. To check for DNA contamination, PCR was run with cDNA samples by using an *L27* (ribosomal housekeeping gene) primer pair, whose PCR product crosses an intron. To check the linearity of detection, a cDNA dilution series (1, 1/10, 1/100, and 1/1000) was amplified with gene-specific primer pairs, and a correlation coefficient was calculated from the standard curve displaying threshold cycles (C_T) as a function of \log_{10} cDNA concentrations (55, 56). The mRNA level for each gene (x) relative to *L27* mRNA (internal control) was calculated as follows: $\text{mRNA}(x\%) = 2^{C_T(L27) - C_T(x)} \times 100$.

Electrophysiology

Whole-cell voltage clamp recordings were performed at room temperature on CAD cells using an EPC 10 amplifier (HEKA Electronics, Germany). Electrodes were pulled from thin-walled borosilicate glass capillaries (Warner Instruments, Hamden, CT) with a P-97 electrode puller (Sutter Instrument, Novato, CA) such that final electrode resistances were 1–2 M Ω when filled with internal solutions. The internal solution for recording Na⁺ currents contained (in mM) 110 CsCl, 5 MgSO₄, 10 EGTA, 4 ATP Na₂-ATP, and 25 HEPES (pH 7.2, 290–310 mOsm/L). The external solution contained (in mM) 100 NaCl, 10 tetraethylammonium chloride (TEA-Cl), 1 CaCl₂, 1 CdCl₂, 1 MgCl₂, 10 D-glucose, 4 4-AP, 0.1 NiCl₂, and 10 HEPES (pH 7.3, 310–315 mOsm/L). Whole-cell capacitance and series resistance were compensated with the amplifier. Series resistance error was always compensated to be less than ± 3 mV. Cells were considered only when the seal resistance was less than 3 M Ω . Linear leak currents were digitally subtracted by P/4.

Lacosamide AB Modification Studies

For experiments designed to determine if lacosamide AB derivatives interacted in a reversible or irreversible manner to affect slow inactivation, the agents (details of concentrations provided in the figure legends) were applied to the CAD cells for 10 min at 37 °C and then washed three times for a total of 5 min at 37 °C prior to whole-cell electrophysiology. The washes (2 mL each) were performed using complete Ham's F12/EMEM medium. Cells were incubated at 37 °C during the washes. Following this washing regimen, the cells were placed in 0.5 mL of extracellular bathing solution for up to 3 min prior to establishing recording seals.

Data Acquisition and Analysis

Signals were filtered at 10 kHz and digitized at 10–20 kHz. Analysis was performed using Fitmaster and origin8.1 (OriginLab Corporation, Northampton, MA). For activation

curves, conductance (G) through Na⁺ channels was calculated using the equation $G = I/(V_m - V_{rev})$, where V_{rev} is the reversal potential, V_m is the membrane potential at which the current was recorded, and I is the peak current. Activation and inactivation curves were fitted to a single-phase Boltzmann function $G/G_{max} = 1/\{1 + \exp[(V - V_{50})/k]\}$, where G is the peak conductance, G_{max} is the fitted maximal G , V_{50} is the half activation voltage, and k is the slope factor. Additional details of specific pulse protocols are described in the results text or figure legends.

Statistical Analyses

Differences between means were compared by unpaired, two-tailed Student's t tests or an analysis of variance (ANOVA), when comparing multiple groups (repeated measures whenever possible). If a significant difference is determined by ANOVA, then a Dunnett's or Tukey's posthoc test was performed. Data are expressed as mean \pm SEM, with $p < 0.05$ considered as the level of significance.

Author Information

Corresponding Author

*E-mail: khanna5@iupui.edu (R.K.); harold_kohn@email.unc.edu (H.K.)

Author Contributions

Y.W. conducted whole cell electrophysiology on CAD cells. K.D.P and C.S. synthesized lacosamide derivatives. S.M.W. performed qRT-PCR and some of the electrophysiology experiments. J.P.S oversaw the whole animal pharmacological studies at the NINDS ASP. R.L. analyzed the data. R.K. and H.K. conceived the study, designed, and supervised the overall project and wrote the manuscript.

Funding Sources

This work is supported by grants from the National Institutes of Health (NIH) (R01NS054112 to H.K., R.L.), the Indiana State Department of Health—Spinal Cord and Brain Injury Fund (A70-9-079138 to R.K.), and the Indiana University Biomedical Committee—Research Support Funds (2286501 to R.K.). S.M.W. is a Stark Scholar.

Notes

The content is solely the responsibility of the authors and does not represent the official views of the National Center for Research Resources, National Institute of Neurological Disorders and Stroke, or the National Institutes of Health. H.K. has a royalty-stake position in (R)-1.

Acknowledgment

We thank Dr. Theodore Cummins (SNRI, Indiana University School of Medicine), members of the Pain and Sensory Group (SNRI, IUSM), Dr. Grant Nicol (IUSM), and Dr. Gerry Oxford (SNRI) for suggestions about analyzing drug-induced IC₅₀ values for slow inactivation and Andrew Piekarcz for comments on the manuscript. We acknowledge the helpful suggestions of the anonymous reviewer regarding use-dependence and kinetics experiments. We thank the

NINDS and the ASP at the National Institutes of Health with Drs. Tracy Chen and Jeffrey Jiang for kindly performing the pharmacological studies via the ASP's contract site at the University of Utah with Drs. H. Wolfe, H.S. White, and K. Wilcox.

Abbreviations

AED, antiepileptic drug; VGSC, voltage-gated Na⁺ channel; AB, affinity bait; CR, chemical reporter; CAD, catecholamine A differentiated; SAR, structure–activity relationship; Na_v1.x, voltage-gated Na⁺ channel isoform 1.x; I_{Na}, Na⁺ current; MES, maximal electroshock; DMTMM, 4-(4,6-dimethoxy-1,3,5-triazin-2-yl)-4-methoxymorpholinium chloride; ASP, Anticonvulsant Screening Program; NINDS, National Institute of Neurological Disorders and Stroke; ip, intraperitoneally; po, orally; ED₅₀, 50% effective dose; TD₅₀, 50% neurological impairment; scMet, subcutaneous Metrazol; qRT-PCR, quantitative reverse transcriptase; CNS, central nervous system; IC₅₀, concentration at which half of the channels have transitioned to a slow inactivated state.

References

1. Hauser, W. A., Annegers, J. F., and Kurland, L. T. (1991) The prevalence of epilepsy in Rochester, Minnesota, 1940–80. *Epilepsia* **32**, 429–445.
2. Evans, J. H. (1962) Post-traumatic epilepsy. *Neurology* **12**, 665–674.
3. Lindsay, J. M. (1971) Genetics and epilepsy. *Epilepsia* **12**, 47–54.
4. Rogawski, M. A., and Porter, R. J. (1990) Antiepileptic drugs: pharmacological mechanisms and clinical efficacy with consideration of promising developmental stage compounds. *Pharmacol. Rev.* **42**, 223–286.
5. Aiken, S. P., and Brown, W. M. (2000) Treatment of epilepsy: existing therapies and future developments. *Front. Biosci.* **5**, E124–152.
6. Brodie, M. J., and Dichter, M. A. (1996) Antiepileptic drugs. *N. Engl. J. Med.* **334**, 168–175.
7. Dichter, M. A., and Brodie, M. J. (1996) New antiepileptic drugs. *N. Engl. J. Med.* **334**, 1583–1590.
8. McNamara, J. O. (2001) in *Goodman's & Gilman's The Pharmacological Basis of Therapeutics* (Hardman, J. G., Limbird, L. E., Eds.) 10th ed., pp 521–547, McGraw-Hill, New York.
9. Kwan, P., and Brodie, M. J. (2000) Epilepsy after the first drug fails: substitution or add-on? *Seizure* **9**, 464–468.
10. Mohanraj, R., and Brodie, M. J. (2006) Diagnosing refractory epilepsy: response to sequential treatment schedules. *Eur. J. Neurol.* **13**, 277–282.
11. McCorry, D., Chadwick, D., and Marson, A. (2004) Current drug treatment of epilepsy in adults. *Lancet Neurol.* **3**, 729–735.
12. Duncan, J. S. (2002) The promise of new antiepileptic drugs. *Br. J. Clin. Pharmacol.* **53**, 123–131.
13. Bauer, J., and Reuber, M. (2003) Medical treatment of epilepsy. *Expert Opin. Emerging Drugs* **8**, 457–467.
14. Mattson, R. H., Cramer, J. A., Collins, J. F., Smith, D. B., Delgado-Escueta, A. V., Browne, T. R., Williamson, P. D., Treiman, D. M., McNamara, J. O., McCutchen, C. B., Homan, R. W., Crill, W. E., Lubozynski, M. F., Rosenthal, N. R., and Mayersdorf, A. (1985) Comparison of carbamazepine, phenobarbital, phenytoin, and primidone in partial and secondarily generalized tonic-clonic seizures. *N. Engl. J. Med.* **313**, 145–151.
15. Pellock, J. M., and Willmore, L. J. (1991) A rational guide to routine blood monitoring in patients receiving antiepileptic drugs. *Neurology* **41**, 961–964.
16. Choi, D., Stables, J. P., and Kohn, H. (1996) Synthesis and anticonvulsant activities of *N*-Benzyl-2-acetamidopropionamide derivatives. *J. Med. Chem.* **39**, 1907–1916.
17. Perucca, E., Yasothan, U., Clincke, G., and Kirkpatrick, P. (2008) Lacosamide. *Nat. Rev. Drug Discovery* **7**, 973–974.
18. Salome, C., Salome-Grosjean, E., Park, K. D., Morieux, P., Swendiman, R., DeMarco, E., Stables, J. P., and Kohn, H. (2010) Synthesis and anticonvulsant activities of (*R*)-*N*-(4-substituted)benzyl 2-acetamido-3-methoxypropionamides. *J. Med. Chem.* **53**, 1288–1305.
19. Morieux, P., Salome, C., Park, K. D., Stables, J. P., and Kohn, H. (2010) The structure-activity relationship of the 3-oxy site in the anticonvulsant (*R*)-*N*-benzyl 2-acetamido-3-methoxypropionamide. *J. Med. Chem.* **53**, 5716–5726.
20. Stohr, T., Kupferberg, H. J., Stables, J. P., Choi, D., Harris, R. H., Kohn, H., Walton, N., and White, H. S. (2007) Lacosamide, a novel anti-convulsant drug, shows efficacy with a wide safety margin in rodent models for epilepsy. *Epilepsy Res.* **74**, 147–154.
21. Errington, A. C., Stohr, T., Heers, C., and Lees, G. (2008) The investigational anticonvulsant lacosamide selectively enhances slow inactivation of voltage-gated sodium channels. *Mol. Pharmacol.* **73**, 157–169.
22. Sheets, P. L., Heers, C., Stoehr, T., and Cummins, T. R. (2008) Differential block of sensory neuronal voltage-gated sodium channels by lacosamide [(2*R*)-2-(acetylamino)-*N*-benzyl-3-methoxypropanamide], lidocaine, and carbamazepine. *J. Pharmacol. Exp. Ther.* **326**, 89–99.
23. Park, K. D., Morieux, P., Salome, C., Cotten, S. W., Reamtong, O., Eysers, C., Gaskell, S. J., Stables, J. P., Liu, R., and Kohn, H. (2009) Lacosamide isothiocyanate-based agents: Novel agents to target and identify lacosamide receptors. *J. Med. Chem.* **52**, 6897–6911.
24. Qi, Y., Wang, J. K. T., McMillian, M., and Chikaraishi, D. M. (1997) Characterization of a CNS line, CAD, in which morphological differentiation is initiated by serum deprivation. *J. Neurosci.* **17**, 1217–1225.
25. Levy, R. H., Mattson, R., and Meldrum, B. (1995) *Antiepileptic Drugs*, 4th ed., pp 99–110, Raven Press, New York.
26. Park, K. D., Stables, J. P., Liu, R., and Kohn, H. (2010) Proteomic searches comparing two (*R*)-lacosamide affinity baits: An electrophilic arylisothiocyanate and a photochemical arylazide group. *Org. Biomol. Chem.* **8**, 2803–2813.

27. de Costa, B. R., Rothman, R. B., Bykov, V., Jacobson, A. E., and Rice, K. C. (1989) Selective and enantiospecific acylation of kappa opioid receptors by (1*S*,2*S*)-trans-2-isothiocyanato-*N*-methyl-*N*-[2-(1-pyrrolidinyl) cyclohexyl] benzeneacetamide. Demonstration of kappa receptor heterogeneity. *J. Med. Chem.* **32**, 281–283.
28. Burke, T. R., Jr., Jacobson, A. E., Rice, K. C., Silverton, J. V., Simonds, W. F., Streaty, R. A., and Klee, W. A. (1986) Probes for narcotic receptor mediated phenomena. 12. cis-(+)-3-Methylfentanyl isothiocyanate, a potent site-directed acylating agent for delta opioid receptors. Synthesis, absolute configuration, and receptor enantioselectivity. *J. Med. Chem.* **29**, 1087–1093.
29. Bayley, H. and Staros, J. V. (1984) *Azides and Nitrenes: Reactivity and Utility*, pp 433–490, Academic Press, Orlando, FL.
30. Bucher, G. (2003) In *CRC Handbook of Organic Photochemistry and Photobiology* (Horspool, W., Lenci, F., Eds.) 2nd ed., pp 1–31, CRC Press, Boca Raton, FL.
31. MacKinnon, A. L., Garrison, J. L., Hegde, R. S., and Taunton, J. (2007) Photo-leucine incorporation reveals the target of a cyclodepsipeptide inhibitor of cotranslational translocation. *J. Am. Chem. Soc.* **129**, 14560–14561.
32. Agard, N. J., Baskin, J. M., Prescher, J. A., Lo, A., and Bertozzi, C. R. (2006) A comparative study of bioorthogonal reactions with azides. *ACS Chem. Biol.* **1**, 644–648.
33. Rostovtsev, V. V., Green, L. G., Fokin, V. V., and Sharpless, K. B. (2002) A stepwise huisgen cycloaddition process: copper(I)-catalyzed regioselective “ligation” of azides and terminal alkynes. *Angew. Chem., Int. Ed.* **41**, 2596–2599.
34. Speers, A. E., Adam, G. C., and Cravatt, B. F. (2003) Activity-based protein profiling in vivo using a copper(I)-catalyzed azide-alkyne [3 + 2] cycloaddition. *J. Am. Chem. Soc.* **125**, 4686–4687.
35. LeTiran, A., Stables, J. P., and Kohn, H. (2002) Design and evaluation of affinity labels of functionalized amino acid anticonvulsants. *J. Med. Chem.* **45**, 4762–4773.
36. Morieux, P., Stables, J. P., and Kohn, H. (2008) Synthesis and anticonvulsant activities of *N*-benzyl (2*R*)-2-acetamido-3-oxysubstituted propionamide derivatives. *Bioorg. Med. Chem.* **16**, 8968–8975.
37. Von Ballmoos, C., Appoldt, Y., Brunner, J., Granier, T., Vassela, A., and Dimroth, P. (2002) Membrane topography of the coupling ion binding site in Na⁺-translocating F1F0 ATP synthase. *J. Biol. Chem.* **277**, 3504–3510.
38. Kunishima, M., Kawachi, C., Monta, J., Terao, K., Iwasaki, F., and Tani, S. (1999) 2-(4,6-Dimethoxy-1,3,5-triazin-2-yl)-4-methyl-morpholinium chloride: An efficient condensing agent leading to the formation of amides and esters. *Tetrahedron* **55**, 13159–13170.
39. Parker, D., and Taylor, R. J. (1987) Direct ¹H NMR assay of the enantiomeric composition of amines and β-amino alcohols using *O*-acetyl mandelic acid as a chiral solvating agent. *Tetrahedron* **43**, 5431–5456.
40. Stables, J. P., and Kupferberg, H. G. (1977) in *Molecular and Cellular Targets for Antiepileptic Drugs* (Avanzini, G., Tanganelli, P., Avoli, M., Eds.), pp 191–198, John Libbey, London.
41. Porter, R. J., Cereghino, J. J., Gladding, G. D., Hessie, B. J., Kupferberg, H. J., Scoville, B., and White, B. G. (1984) Antiepileptic drug development program. *Cleveland Clin. Q.* **51**, 293–305.
42. Dunham, N. W., and Miya, T.-S. (1957) A note on a simple apparatus for detecting neurological deficit in rats and mice. *J. Am. Pharm. Assoc.* **46**, 208–209.
43. White, H. S., Woodhead, J. H., Wilcox, K. S., Stables, J. P., Kupferberg, H. J., and Wolf, H. H. (2002) General Principles: Discovery and Preclinical Development of Antiepileptic Drugs, in *Antiepileptic Drugs* (Levy, R. H., Mattson, R. H., Meldrum, B. S., Perruca, E., Eds.) 5th ed., pp 36–48, Lippincott, Williams and Wilkins, Philadelphia.
44. Swinyard, E. A. (1969) Laboratory evaluation of anti-epileptic drugs: review of laboratory methods. *Epilepsia* **10**, 107–119.
45. Wang, H., and Oxford, G. S. (2000) Voltage-dependent ion channels in CAD cells: A catecholaminergic neuronal line that exhibits inducible differentiation. *J. Neurophysiol.* **84**, 2888–2895.
46. Wang, Y., Brittain, J. M., Jarecki, B. W., Park, K. D., Wilson, S. M., Wang, B., Hale, R., Meroueh, S. O., Cummins, T. R., and Khanna, R. (2010) In silico docking and electrophysiological characterization of lacosamide binding sites on collapsin response mediator protein-2 identifies a pocket important in modulating sodium channel slow inactivation. *J. Biol. Chem.* **285**, 25296–25307.
47. Rudy, B. (1978) Slow inactivation of the sodium conductance in squid giant axons. Pronase resistance. *J. Physiol.* **283**, 1–21.
48. Hodgkin, A. L., and Huxley, A. F. (1952) The dual effect of membrane potential on sodium conductance in the giant axon of Loligo. *J. Physiol.* **116**, 497–506.
49. Bean, B. P. (2007) The action potential in mammalian central neurons. *Nat. Rev. Neurosci.* **8**, 451–465.
50. Do, M. T., and Bean, B. P. (2003) Subthreshold sodium currents and pacemaking of subthalamic neurons: modulation by slow inactivation. *Neuron* **39**, 109–120.
51. Vilin, Y. Y., and Ruben, P. C. (2001) Slow inactivation in voltage-gated sodium channels: molecular substrates and contributions to channelopathies. *Cell Biochem. Biophys.* **35**, 171–190.
52. Catterall, W. A. (2002) Molecular mechanisms of gating and drug block of sodium channels. *Novartis Found. Symp.* **241**, 206–218, discussion 218–232.
53. Song, Z., and Zhang, Q. (2009) Fluorous aryldiazirine photoaffinity labeling reagents. *Org. Lett.* **11**, 4882–4885.
54. Brittain, J. M., Piekarczyk, A. D., Wang, Y., Kondo, T., Cummins, T. R., and Khanna, R. (2009) An atypical role for collapsin response mediator protein 2 (CRMP-2) in neurotransmitter release via interaction with presynaptic voltage-gated Ca²⁺ channels. *J. Biol. Chem.* **284**, 31375–31390.
55. Kondo, T., Johnson, S. A., Yoder, M. C., Romand, R., and Hashino, E. (2005) Sonic hedgehog and retinoic acid synergistically promote sensory fate specification from bone

marrow-derived pluripotent stem cells. *Proc. Natl. Acad. Sci. U.S.A.* *102*, 4789–4794.

56. Kondo, T., Sheets, P. L., Zopf, D. A., Aloor, H. L., Cummins, T. R., Chan, R. J., and Hashino, E. (2008) Tlx3 exerts context-dependent transcriptional regulation and promotes neuronal differentiation from embryonic stem cells. *Proc. Natl. Acad. Sci. U.S.A.* *105*, 5780–5785.

57. Kuo, C.-C., and Bean, B. P. (1994) Slow binding of phenytoin to inactivated sodium channels in rat hippocampal neurons. *Mol. Pharmacol.* *46*, 716–725.